



Electronic spectra and molecular geometry of the non-linear carbon chain C_9H_3

D. Zhao^{a,*}, N. Wehres^{b,c}, H. Linnartz^{a,c}, W. Ubachs^a

^a Institute for Lasers, Life and Biophotonics, VU University Amsterdam, De Boelelaan 1081, NL 1081 HV Amsterdam, The Netherlands

^b Kapteyn Astronomical Institute, University of Groningen, P.O. Box 800, NL 9700 AV Groningen, The Netherlands

^c Raymond and Beverly Sackler Laboratory for Astrophysics, Leiden Observatory, Leiden University, P.O. Box 9513, NL 2300 RA Leiden, The Netherlands

ARTICLE INFO

Article history:

Received 20 September 2010

In final form 15 November 2010

Available online 18 November 2010

ABSTRACT

Two electronic bands at ~ 18881 and ~ 18920 cm^{-1} – previously assigned to the carbon chain molecule C_9H_3 – have been recorded, resolving for the first time their K-stack structure. The C_9H_3 radicals are produced by discharging and expanding a diluted gas mixture of acetylene in helium employing a pulsed pinhole nozzle. Cavity ring-down spectroscopy is used to record spectra in direct absorption. The improved experimental data and spectrum simulations based on new theoretical structure predictions show that the $HC_4(CH)C_4H$ isomer (with C_{2v} symmetry) is a likely carrier of the two observed C_9H_3 bands.

© 2010 Elsevier B.V. All rights reserved.

1. Introduction

In the last three decades many studies have been dedicated to the formation, spectral characterization and identification of carbon chain species of the form $X_mC_nY_y^{(+/-)}$, with typically $X, Y = H, N, O$ and S . These unsaturated species are important constituents in plasma environments, and have been found to be well represented in the interstellar medium (see [1–3] and references cited therein). Carbon chains as large as $HC_{11}N$ and carbon chain cat- and anions have been identified in dense interstellar clouds by comparing radio astronomical and microwave laboratory spectra [4,5]. Rovibrationally resolved infrared spectra have been recorded in the gas phase particularly for pure and bare carbon chains, C_n , with C_{13} the largest system studied so far [6]. Optical gas phase spectra of carbon chains have been obtained using a range of experimental techniques, including REMPI-TOF, photo-detachment, degenerate 4-wave mixing, and ion trap schemes [7] as well as cavity ring-down and plasma-frequency double modulation spectroscopy (see Refs. [7,8]). The resulting spectra have provided insight in the electronic nature of these species and have been used for comparisons with optical absorption spectra observed through translucent interstellar clouds to search for potential carriers of the so called diffuse interstellar bands [7–9].

The majority of the carbon chain radicals that have been studied so far is linear, but several families of non-linear carbon chains have been reported [10–14]. In this Letter the focus is on the optical spectroscopy of C_9H_3 . This species is a member of the $C_{2n+1}H_3$ family that has been observed for $n = 3 – 6$ in a mass selective REMPI-TOF experiment [10–12]. Schmidt and coworkers found

that the origin bands of the C_9H_3 , $C_{11}H_3$ and $C_{13}H_3$ all absorbed in a rather narrow wavelength range, between 520 nm and 530 nm. As absorption frequencies typically shift to the red with increasing chain length [15] the authors suggested that this ‘un-chain-like’ behaviour could be due to a ring-chain motif. The absence of clear rotational information, however, precluded a definitive determination of the geometrical structure.

Density functional theory (DFT) calculations by Zhang [13] predicted the structure, stability and electronic transitions of $C_{2n+1}H_3$ for $n = 4 – 6$. From this study it was concluded that the molecular geometry of the C_9H_3 carrier of the REMPI-TOF laboratory spectrum [11] does not incorporate a carbon ring and that a non-linear bent structure is the more likely carrier of the experimental spectrum. The present study contributes to this discussion with improved experimental results providing for the first time resolved K-stack spectra for two previously observed electronic bands.

2. Experimental

The experiment is based on a pulsed cavity ring-down detection scheme that has been described in detail previously [8,16]. The C_9H_3 radicals are produced in a supersonically expanding hydrocarbon plasma by discharging a 0.5% C_2H_2/He mixture. The present experiment employs a pinhole discharge nozzle connected to a pulsed valve system (General Valve series 9), and is a modified version of the pinhole system described in Ref. [17] to generate transient species at low final rotational temperatures. The modifications are essential in order to realize the improvements necessary to record a K-stack resolved spectrum. More specifically, the present nozzle geometry comprises four separated layers – two metal plates and two ceramic plates – which act as electrodes and insulators, as shown in Figure 1. In the modified system, the diameter of

* Corresponding author. Fax: +31 20 5987999.

E-mail address: d.zhao@vu.nl (D. Zhao).

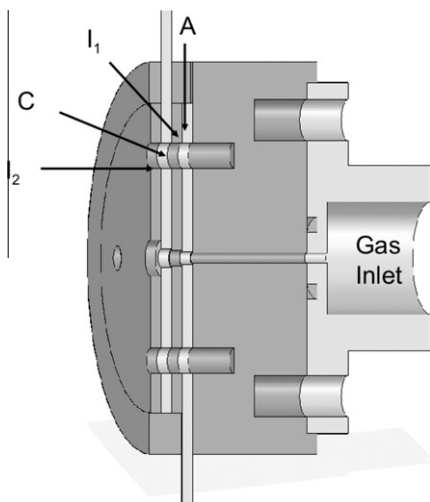


Figure 1. Schematic view of the pinhole nozzle. The ceramic body is mounted to a pulsed valve system that runs at 10 Hz and provides a gas pulse that is discharged by applying a negative high voltage pulse (-1000 V) to the cathode (C), striking upstream towards the grounded anode (A). The two plates are isolated by ceramic insulators ($I_{1,2}$). The plates have a thickness of ($A/I_1/C/I_2 = 1.0, 0.8, 1.0$ and 2.0 mm) and the diameter of the central holes is increasing downstream: ($A/I_1/C/I_2 = 1.0, 1.5, 1.8$ and 3.5 mm).

the central hole in each plate increases from 1.0 to 3.5 mm towards the orifice. The smaller distance between the anode and cathode effectively increases the current density in the discharge region. The final ceramic plate (I_2) has a hole with a diameter of ~ 3.5 mm and is used to prevent the discharge from clogging. The ~ 2 mm thickness of this plate narrows the jet expansion angle, enhancing the collisional rate in the jet and decreasing the Doppler broadening. The nozzle is mounted in a vacuum chamber, that is evacuated by a roots-blower pump system with 1000 m³/h pumping capacity. The typical pressure is ~ 0.03 mbar in the chamber during jet operation for a backing pressure of ~ 7 bar.

Tunable laser pulses are generated by a pulsed dye laser (Sirah, Cobra Stretch) pumped by a frequency tripled Nd:YAG laser operated at a 10 Hz repetition rate with a pulse width of ~ 6 ns and a bandwidth narrower than 0.04 cm⁻¹. Convoluting this value with an estimated Doppler width of ~ 0.05 cm⁻¹ results in a spectral resolution of ~ 0.07 cm⁻¹. The absolute laser frequency is calibrated with a precision better than 0.02 cm⁻¹ using an iodine absorption reference spectrum that is recorded simultaneously. Cavity ring-down events are obtained by injecting a fraction of the laser pulse into a high-finesse optical cavity, which consists of two plano-concave mirrors (Research Electro-Optics, reflectivity $\sim 99.998\%$ at 532 nm) that are mounted on high precision alignment tools. The cavity length is ~ 58 cm, yielding typical ring-down times of 60–80 μ s. A multi trigger scheme is used to match the ring-down event to the gas pulse (~ 1 ms) and the coinciding discharge pulse (~ 300 μ s and -1000 V). The optical axis of the cavity crosses the plasma expansion perpendicularly. The distance of the cavity axis to the nozzle orifice can be varied during jet operation from 0 to 20 mm. Spectra are recorded for three different distances at $\sim 2, 7$ and 12 mm and the ongoing adiabatic cooling causes the rotational temperature to drop, yielding $T_{rot} \sim 23, \sim 14$ and ~ 7 K, respectively. The light leaking out of the cavity traverses a narrow bandpass filter before it is detected by a photomultiplier tube (PMT). The PMT signal is digitized by an oscilloscope and the obtained data is transferred to a computer. The ring-down signal is analysed in real time by a LABVIEW program. Typically 6–10 ring-down events are averaged to determine one data point. A full spectrum is obtained by recording the averaged ring-down time as a function of laser frequency.

3. Results and discussion

3.1. Experimental spectra and analysis

In panel (a) of Figure 2 the electronic origin band spectrum of C₉H₃ is shown, recorded around 18881 cm⁻¹. The unambiguous assignment of this rotationally unresolved band to this specific molecular formula follows from a previous mass selective REMPI-TOF study [10,11]. The spectrum consists of a P- and R-branch. The P-branch exhibits a clear K-stack-resolved structure. The individual K-stacks making up the spectrum are shown as individual stick diagrams (panel (b)) and are discussed in more detail later. Several partially resolved peaks in the R-branch have spacings of ~ 0.11 cm⁻¹ (zoom-in) and are the cumulative result of a series of coinciding rotational transitions starting from $K_a = 0-6$.

The clearly resolved K-stack progression ($K_a = 0-12$) in the P-branch is typical for a non-linear molecule. The incremental spacing between neighbouring K-stacks towards the low frequency side indicates that the underlying electronic transition should be parallel and that the observed spectrum reflects an A-type transition. Indeed, using the PGOPHER software [18], a contour fitting for an A-type transition using an asymmetric top model and C_s symmetry reproduces the observed spectrum well. This empirical contour fitting yields indicative values of the molecular constants: $T_0 \approx 18881.4$ cm⁻¹, $A'' \approx 0.215$ cm⁻¹, $B'' \approx C'' \approx 0.0159$ cm⁻¹, and $\Delta(A - (B + C)/2) \approx -0.0181$ cm⁻¹.

Besides the origin band a transition to a vibronically excited state is observed around 18920 cm⁻¹ (Figure 3). The transition, only 39 cm⁻¹ blue shifted, was also detected at lower resolution in the previously mentioned REMPI-TOF experiment and assigned to an electronic transition of C₉H₃, involving excitation of a low lying bending mode in the upper electronic state. The spectrum recorded here has a similar contour as the origin band at 18881 cm⁻¹, and exhibits a very similar K-stack resolved structure. It is likely that this transition is due to the excitation of the same isomeric C₉H₃ form and that the excited state corresponds to a completely symmetric vibrational mode (a_1 or a' symmetry) with an energy of about 39 cm⁻¹. In Figure 3 a contour fit is shown based on similar rotational constants as used for the origin band transition in Figure 2.

3.2. Consideration of the molecular geometry

DFT calculations at the B3LYP/6-31G* level have been reported in Ref. [13] for a large set of possible C₉H₃ isomers, yielding their geometry, stability and vibrational frequencies. Our estimated values for the molecular constants, $A'' \approx 0.215$ cm⁻¹ and $B'' \approx C'' \approx 0.0159$ cm⁻¹, derived from the band contour fitting, are very close to the calculated rotational constants of the A3 and A7 isomers (Table 2 of Ref. [13], see also Figure 4) with C_{2v} and C_s symmetry, respectively. The other geometries listed in Ref. [13] are for transition states or have molecular constants that substantially deviate from the values estimated here, and are not further considered.

A ring-chain motif (like A7) was suggested by Schmidt et al. [10,11] based on REMPI spectra and electronic structure calculations [12] and the observation that the longer chains C₁₁H₃ and C₁₃H₃ also absorb in the 520–530 nm region, i.e., do not substantially red shift with respect to C₉H₃. In Ref. [11] the authors argue that C₉H₃ should have a low IP (≤ 6.4 eV), as the corresponding mass 111 amu was found to be the most abundant ion upon the irradiation of the products of a butadiyne/Ar discharge with a 193 nm (6.4 eV) laser. The DFT calculations performed in the present work (Table 1) indicate that the ionization potential of the A3 isomer amounts to 7.6 eV, which is somewhat lower than the total photon energy of ≤ 8.2 eV used in the (1 + 1') REMPI measurement

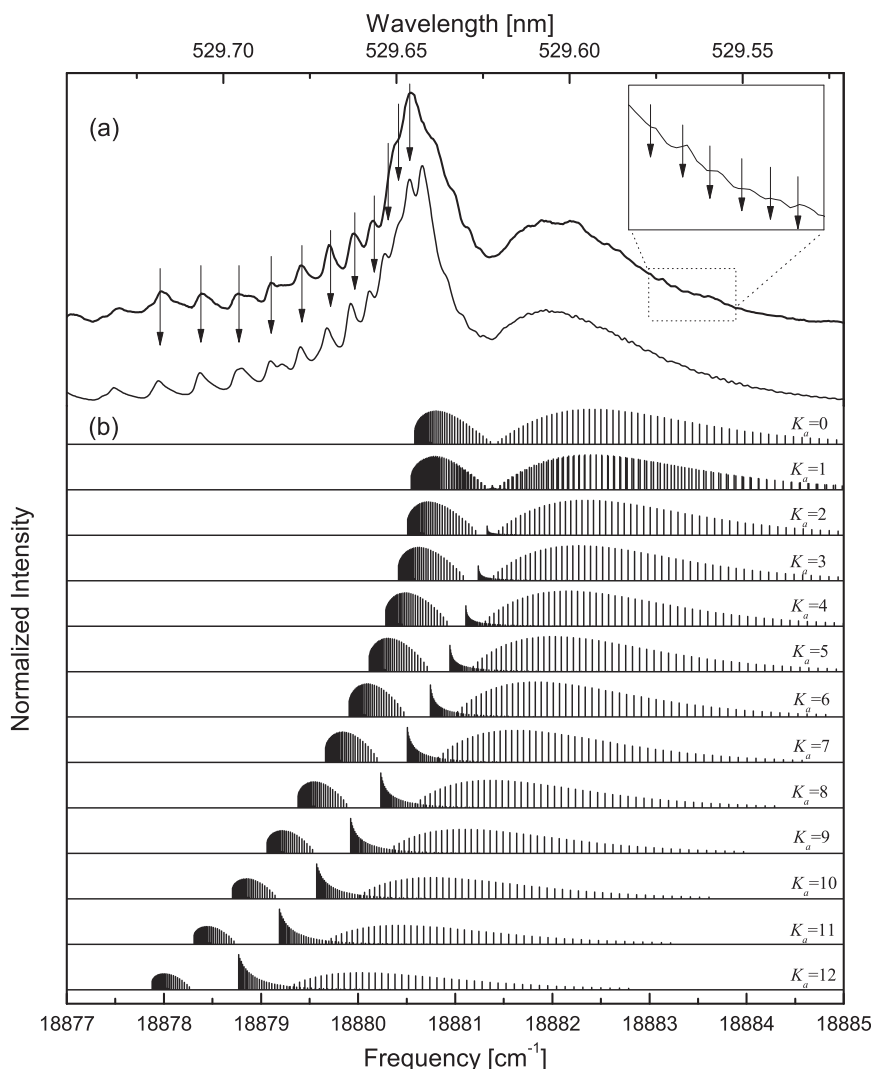


Figure 2. The experimentally obtained electronic origin band spectrum of C_9H_3 . The upper trace of panel (a) shows the K-stack resolved spectrum. The arrows indicate the unresolved band heads of the subbands ($K_a = 0-12$). The inset in panel (a) represents a zoom-in of the partially rotationally resolved R-branch (see also Figure 5). The lower trace of panel (a) indicates an empirical contour fit (with a GAUSSIAN linewidth of 0.07 cm^{-1}) to derive approximate rotational constants. Panel (b) shows the simulated stick diagrams for the individual subbands. The rotational temperature derived from the simulation is $\sim 23\text{ K}$.

[10], but larger than the appearance potential of the C_9H_3 mass determined from the irradiation experiment. The calculated IPs of the ring-bearing isomers (e.g., 6.34 eV for isomer A7) are smaller and agree with the experimental appearance potential for mass 111 amu. A consistent explanation for this discrepancy is that the butadiyne/Ar discharge actually does produce the isomer A7, but since the experiment only uses mass detection, this result does not necessarily link the IP value of the carrier to the actual spectra observed by Schmidt and co-workers. The DFT work [13], however, proposed the A3 isomer as the more likely carrier of the C_9H_3 bands, based on minimum energy considerations. The present work adds to this discussion with improved experimental spectra and additional calculations. The latter have been performed only for the two selected C_9H_3 isomers A3 and A7, using the GAUSSIAN 98 software package [19] and an extended basis set B3LYP/6-311G^{**}. The calculated geometries and structural parameters are close to the values found in Ref. [13] and indicated in Figure 4. The resulting rotational frequencies and the ionization potentials (IPs) are listed in Table 1.

It is clear from the discussion above that the resolved K-stack structure alone is not sufficient to discriminate between the A3

and A7 isomeric forms, since both species result in a spectrum that is very similar to the one shown in Figure 2. Additional arguments are needed to select one of the two isomers as the likely carrier of the bands observed here and reported in Ref. [10]. These arguments are systematically discussed below.

(I) The DFT calculations, both in Ref. [13] and in the present study, find an A7 minimum energy that is higher (1.27 and 1.29 eV, respectively) than the A3 minimum energy value. This favors – from a pure theoretical point of view – the C_{2v} bent isomer geometry as the more likely carrier of the observed spectra. In a reactive plasma environment with much excess energy, one should be careful to eliminate less stable configurations, on the basis of a minimum energy argument only. However, as no other obvious C_9H_3 features pertaining to another isomer have been observed in the REMPI work [11], it is likely that the present bands arise from the minimum energy configuration.

(II) The DFT calculations show that both isomers are expected to have a completely symmetric vibrational mode with a low excitation energy in their electronic ground state: 43 cm^{-1} (a_1) for the A3 isomer and 57 cm^{-1} (a') for the A7 isomer. For most larger carbon chains it is found that upon electronic excitation the molecular geometry barely changes [20,21] and the vibrational spacings in

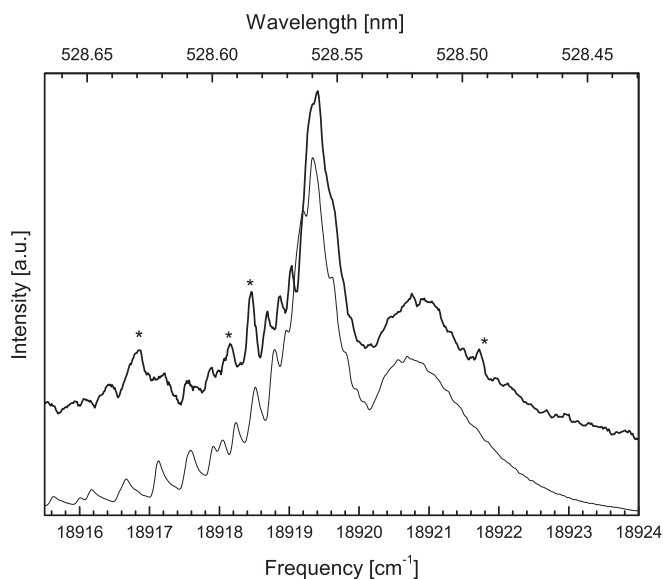


Figure 3. The experimentally obtained C_9H_3 absorption spectrum (bold line) of an electronic transition involving a vibrationally excited state in the upper electronic state, about 39 cm^{-1} blue shifted with respect to the origin band transition. The asterisks indicate overlapping transitions of smaller species, including C_2 and C_2^- . A contour fit (regular line) of the spectrum is also plotted based on constants as used for the origin band transition.

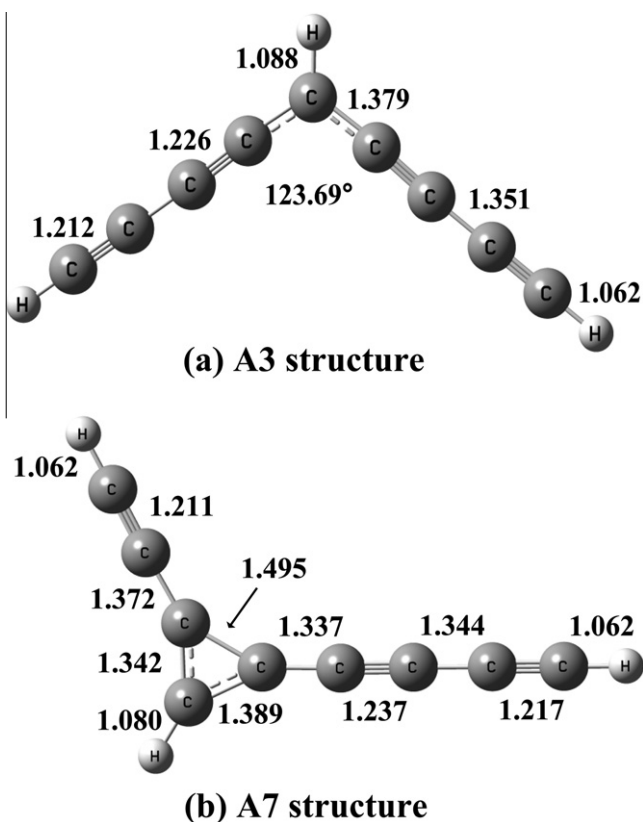


Figure 4. The geometry of the A3 and A7 isomers as introduced in Ref. [13] are shown. The bond lengths (in angstrom) and the angle of the bend C_{2v} structure result from improved calculations at the DFT-B3LYP/6-311G^{**} level (Table 1). The likely carrier of the spectra shown in Figs. 2 and 3 is isomer A3.

the first excited electronic state are therefore expected to be comparable to those in the ground state. The calculations of the isomer A3 at the B3LYP/6-31G^{*} level in Ref. [13] show that the bond

Table 1

Molecular parameters of the C_9H_3 A3 and A7 isomers compared to DFT calculations at the B3LYP/6-31G level from Ref. [13].

Isomer	A3 [C_{2v}]		A7 [C_s]		Expt.
	6-311G ^{**a}	6-31G ^{*b}	6-311G ^{**a}	6-31G ^{*b}	
ΔE (eV)	0	0	1.29	1.27	
A'' (cm^{-1})	0.22683	0.21892	0.17980	0.17988	
B'' (cm^{-1})	0.016377	0.01637	0.020562	0.02039	
C'' (cm^{-1})	0.015274	0.01523	0.018452	0.01831	
ν_{39} (cm^{-1})	43.4(a_1)	45(a_1)	56.5(d')	60(d')	38.8 ^c
IP (eV)	7.6		6.34		<8.2 ^d

^a This work.

^b Ref. [13].

^c Value for the upper state, derived from the band origin values (T_0) in Table 2.

^d The total photon energy of the (1 + 1') REMPI experiment [10,11].

lengths and bond angle(s) indeed do not show significant changes between the ground and excited states. Consequently, the experimentally observed blue shift of the band at 18920 cm^{-1} with respect to the origin band offers a selection criterium. The experimental value of 38.8 cm^{-1} for the excited state bending mode is closer to the predicted 43 cm^{-1} value calculated for the A3 ground state geometry than for the corresponding A7 geometry (57 cm^{-1}).

(III) Although the simulations for both isomers reproduce the contour of the observed spectra reasonably well, only the simulation for the A3 isomer exhibits a similar profile of the partially resolved (and reproducible) rotational structure in the R-branch (inset Figures 2 and 5). The simulated high-resolution spectra (using a GAUSSIAN linewidth of 0.02 cm^{-1} in the simulations) indicate that the R-branch of the spectrum of the A7 isomer (C_s symmetry) will resolve lines with spacings of about 0.06 cm^{-1} , whereas the spacings are about 0.11 cm^{-1} in the A3 isomer (C_{2v} symmetry) spectrum, which is very close to the actually observed values. The two times larger spacing in the symmetric isomer A3 spectrum arises from the 1:3 intensity alternation of odd and even K_b values due to nuclear spin statistics. This is illustrated in Figure 5, where also simulations are presented at the actual spectral resolution of 0.07 cm^{-1} . The A3 simulation is clearly closer to the experimental spectrum than the A7 simulation, but more importantly, even though this rotational progression is the cumulative result of a series of individual and overlapping rotational transitions, a spacing of 0.11 cm^{-1} cannot be realized with individual transitions being separated by 0.06 cm^{-1} . I.e., this part of the spectrum conflicts with the A7 geometry.

Arguments II and III hint for the bent C_{2v} structure as the molecular carrier of the observed spectrum and are fully consistent with argument I.

Additional experiments can be performed. We have tried to distinguish between both isomers by searching for spectral differences as a function of rotational temperature. For this measurements have been performed at different distances downstream in the expansion. Empirical contour fittings were performed, using the ground state rotational constants derived from the DFT calculations here. The simulated spectra for both isomers A3 and A7 are plotted and compared to the experimental spectra in Figure 6. The plots show that the experimentally obtained spectra for the origin band transition (left panel) and the excited mode (right panel) can be reproduced both for the A3 (upper spectrum) and A7 (lower spectrum) constants, but unfortunately from this no conclusive information can be obtained on the actual carrier.

The rotational structure of the recorded spectrum is not resolved, therefore a rotational contour fit [18], utilizing a least squares procedure is needed to fit the overall shape of the experimental spectrum. This method has been used previously to analyze

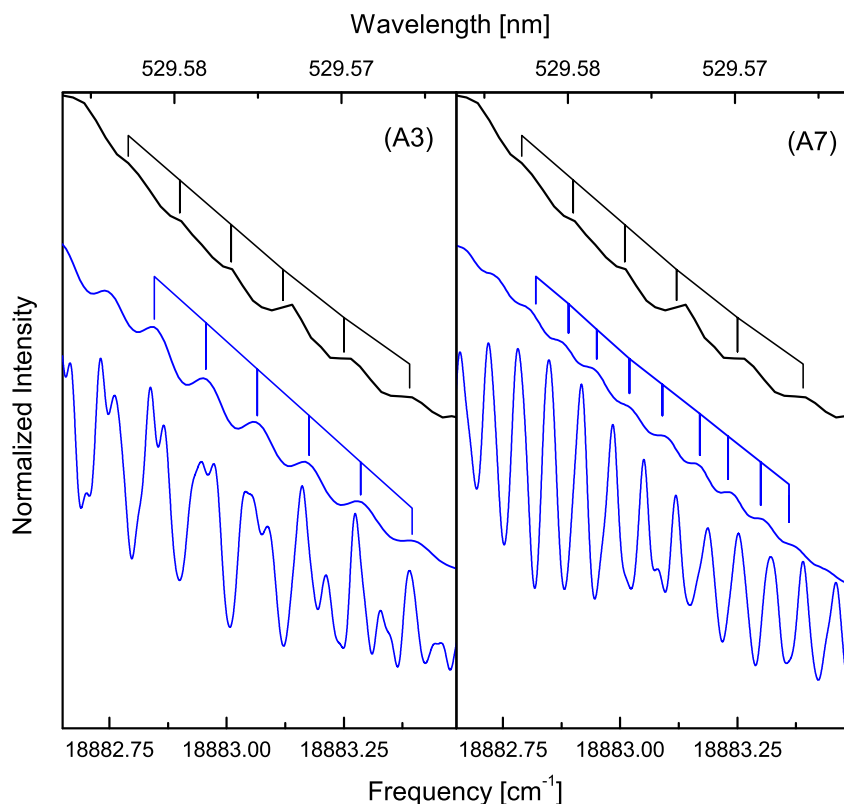


Figure 5. The partially resolved rotational structure in the R-branch (inset Figure 1) and simulated spectra for the A3 isomer with C_{2v} symmetry and 1:3 spin statistical weights (left panel) and the A7 isomer with C_s symmetry and no spin statistical weights (right panel). The upper bold line gives the experimental spectrum (and is identical in both plots). The bottom spectrum shows the simulation for 0.07 cm^{-1} linewidth to visualize the underlying spin statistics. The middle trace is the resulting spectrum for a linewidth of 0.07 cm^{-1} (comparable to the experimental resolution).

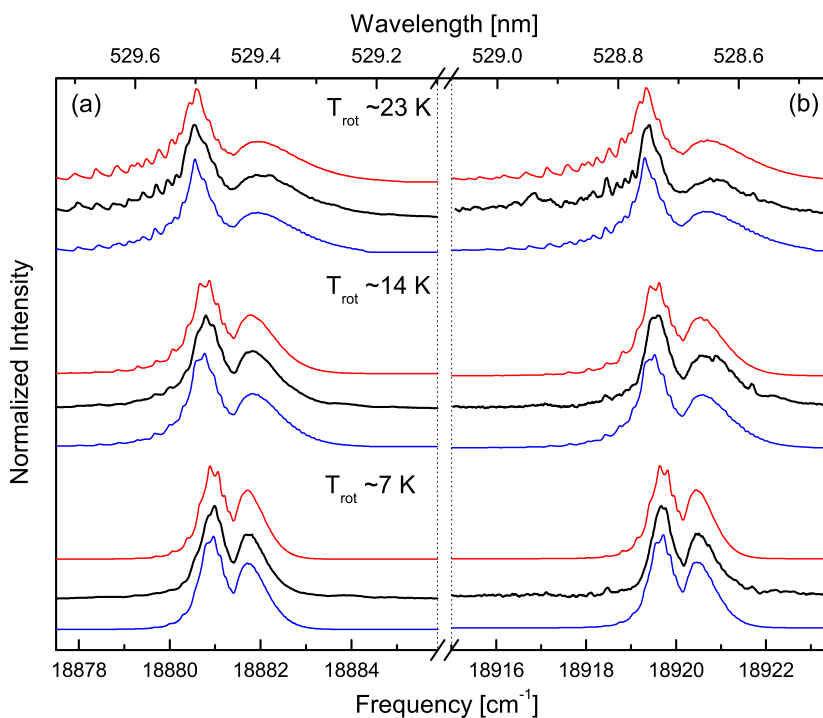


Figure 6. The experimental spectra of the two C_9H_3 bands recorded for three different rotational temperatures: $\sim 23\text{ K}$ (2 mm), $\sim 14\text{ K}$ (7 mm) and $\sim 7\text{ K}$ (12 mm). The experimental spectra are represented by a bold black line and compared to the simulated spectrum for the A3 (A7) geometry and are plotted above (below) the experimental spectra.

the spectra of other non-linear carbon chains, like $\text{trans-C}_6\text{H}_4^+$ [20], $C_6H_3^+$, and $C_8H_3^+$ [21]. Here a similar procedure is followed assum-

ing that the spectrum of an asymmetric molecule is characterized by the rotational constants A, B and C in both states, the band

Table 2
Inferred molecular constants (cm^{-1}) for the two C_9H_3 bands discussed here.

	~ 18881 cm^{-1}	~ 18920 cm^{-1}
T_0	18881.41(1) ^a	18920.21(1) ^a
A''^b	0.22683	0.22683
B''^b	0.016377	0.016377
C''^b	0.015274	0.015274
A'	0.20925(3) ^c	0.20917(7) ^c
B'	0.01667(1) ^c	0.01666(3) ^c
C'	0.01555(1) ^c	0.01554(3) ^c
$\Delta(A - (B + C)/2)^d$	-0.01787	-0.01794
A''/A'	1.082	1.084
B''/B'^e	0.982	0.982

^a The errors represent the statistical uncertainties as obtained in the least squares fit.

^b Fixed to the calculated values of isomer A3 (this work).

^c Errors are determined by a least squares fit of the resolved K-stacks at a rotational temperature of ~ 23 K.

^d $\Delta(A - (B + C)/2) = (A' - (B' + C')/2) - (A'' - (B'' + C'')/2)$.

^e Assuming that $B''/B' \approx C''/C'$.

origin, and the full-width-at-half-maximum (FWHM, $\sim 0.07 \text{ cm}^{-1}$) of a GAUSSIAN line profile. The rotational constants in the ground state are fixed using the results of isomer A3 from the new DFT calculations at the B3LYP/6-311G^{**} level. Furthermore the rotational temperature is fixed using the estimated values from the empirical contour fit. That way the rotational contour fit yields the band origin and the spectroscopic constants for the upper state. The results are summarized in table 2.

In a similar way, the spectrum of the vibronic band around 18920 cm^{-1} is reproduced through a contour fit using the calculated ground state constants of isomer A3 and the same A-type transition. This is shown in Figure 3. It is found that the resulting ratios of A''/A' and B''/B' for both the 18881 and 18920 cm^{-1} bands, are close to unity, in agreement with the assumption made under point II that the molecular structure will not substantially change upon electronic excitation.

All arguments given above, based on the new observations and calculations presented here, are consistent in that they point towards the A3 isomer as the more likely carrier of the observed

laboratory spectra. Clearly, the pure rotational spectrum of the isomer A3 would settle the issue, and may be measured in a Fourier transform microwave experiment [1] or by linking the pure rotational spectrum to the electronic spectrum presented here in a microwave-optical double resonance experiment [22].

Acknowledgements

We acknowledge the financial support provided by the Foundation for Fundamental Research of Matter (FOM) and by NOVA, the Netherlands Research School for Astronomy, as well as the Marie Curie FP6 Network “The Molecular Universe”. We thank Prof. A.G.G.M. Tielens for stimulating discussions.

References

- [1] P. Thaddeus, M.C. McCarthy, M.J. Travers, C.A. Gottlieb, W. Chen, *Faraday Discuss. Chem. Soc.* 109 (1998) 121.
- [2] A.G.G.M. Tielens, *The Physics and Chemistry of the Interstellar Medium*, Cambridge University Press, Cambridge, 2005.
- [3] V. Wakelam et al., *Space Sci. Rev.* (2010). arXiv:1011.1184v1 [astro-ph.GA].
- [4] M.B. Bell, P.A. Feldman, M.J. Travers, M.C. McCarthy, C.A. Gottlieb, P. Thaddeus, *Astrophys. J.* 483 (1997) L61.
- [5] S. Brunken, H. Gupta, C.A. Gottlieb, M.C. McCarthy, P. Thaddeus, *Astrophys. J.* 664 (2007) L43.
- [6] T.F. Giesen, A. Van Orden, H.J. Hwang, R.S. Fellers, R.A. Provencal, R.J. Saykally, *Science* 265 (1994) 756.
- [7] E.B. Jochowitz, J.P. Maier, *Ann. Rev. Phys. Chem.* 59 (2008) 519.
- [8] H. Linnartz, in: G. Berden, R. Engeln (Eds.), *Cavity Ring-Down Spectroscopy – Techniques and Applications*, Wiley-Blackwell, 2009, p. 145.
- [9] A.G.G.M. Tielens, T.P. Snow, *The Diffuse Interstellar Bands*, Kluwer Academic Publishers, Dordrecht, 1995.
- [10] T.W. Schmidt, H. Ding, A.E. Boguslavskiy, T. Pino, J.P. Maier, *J. Phys. Chem. A* 107 (2003) 6550.
- [11] T.W. Schmidt, A.E. Boguslavskiy, T. Pino, H. Ding, J.P. Maier, *Int. J. Mass. Spectr.* 228 (2003) 647.
- [12] H. Ding, T. Pino, F. Güthe, J.P. Maier, *J. Am. Chem. Soc.* 125 (2003) 14626.
- [13] C. Zhang, *J. Chem. Phys.* 121 (2004) 8212.
- [14] M.C. McCarthy, P. Thaddeus, *Chem. Soc. Rev.* 30 (2001) 177.
- [15] J.P. Maier, *Chem. Soc. Rev.* 26 (1997) 21.
- [16] N. Wehres, D. Zhao, H. Linnartz, W. Ubachs, *Chem. Phys. Lett.* 497 (2010) 30.
- [17] G. Bazalgette Courrèges-Lacoste, J.P. Sprengrs, J. Bulthuis, S. Stolte, T. Motylewski, H. Linnartz, *Chem. Phys. Lett.* 335 (2001) 209.
- [18] C.M. Western, 2007, University of Bristol, <<http://pgopher.chm.bris.ac.uk>>.
- [19] M.J. Frisch, G.W. Trucks, H.B. Schegel et al., *GAUSSIAN 98*, Gaussian Inc., Pittsburgh, PA, 1998.
- [20] M. Araki et al., *J. Chem. Phys.* 118 (2003) 10561.
- [21] A. Dzhonson, E.B. Jochowitz, E. Kim, J.P. Maier, *J. Chem. Phys.* 126 (2007) 044301.
- [22] M. Nakajima, Y. Sumiyoshi, Y. Endo, *Rev. Sci. Instrum.* 73 (2002) 165.